Predicting Total Ozone Based on GTS Data: Applications for South American High-Latitude Populations

ANNA E. JONES, TANYA BOWDEN,* AND JOHN TURNER

British Antarctic Survey, Natural Environment Research Council, Cambridge, United Kingdom

(Manuscript received 6 January 1997, in final form 1 September 1997)

ABSTRACT

A regular occurrence during the 1990s has been the excursion of the edge of the springtime Antarctic ozone hole over the southernmost region of the South American continent. Given the essential role of atmospheric ozone in absorbing incoming solar ultraviolet radiation, the populations in this area are thus exposed to much higher ultraviolet-B irradiance than is normal for this time of year. The authors report here on a simple technique that might be used to forecast these low ozone episodes, based upon data readily available on the World Meteorological Organization Global Telecommunications System. Using this technique, total ozone during October 1991 at Punta Arenas, Chile, is predicted with a root-mean-square error of 34.4 DU (12.8%) and a mean error of 14.8 DU (5.5%).

1. Introduction

It is well documented that the ultraviolet (UV) component of solar radiation, particularly that between 280 and 315 nm (UV-B), has the potential to cause cell damage to both plants and animals (Karentz 1994). The intensity of UV-B radiation that reaches the earth's surface depends primarily upon the solar zenith angle, the amount of cloud cover, and the total ozone column (Gautier et al. 1994). The strong anticorrelation between total ozone and UV irradiance has been demonstrated unambiguously from clear-sky observations made at the South Pole (Booth et al. 1994). The change in UV irradiance arising from a reduction in total column ozone varies with wavelength, increasing significantly toward shorter wavelengths. The DNA-effective irradiances, at the very short UV-B wavelengths, are thus strongly sensitive to changes in the column ozone amount (Setlow 1974). Other factors such as aerosol loading and surface albedo also play a role in moderating the incident UV irradiation (McKenzie et al. 1995).

During late spring, the populations of southern South America are usually protected from incoming solar UV-B radiation by the circumpolar warm belt, the region of high ozone situated equatorward of the polar vortex. Regular ground-based measurements of total ozone made with a Brewer spectrophotometer by the University of Magallenes, Punta Arenas, Chile, show that during October, for example, the climatological average column ozone amount is 345 DU over Punta Arenas (53.1°S, 70.6°W) (Kirchhoff et al. 1997). However, over recent years, with the increase in size of the Antarctic ozone hole, large distortions of the vortex have resulted in the edge of the ''hole'' moving periodically across this region. Consequently, the lowest daily value of total column ozone measured by the Brewer at Punta Arenas was 145.8 DU, recorded on 17 October 1994 (Kirchhoff et al. 1997). The extension of the hole over Punta Arenas on this occasion can clearly be seen from Total Ozone Mapping Spectrometer (TOMS) data, as shown in Fig. 1.

The highest UV irradiances in the Antarctic do not necessarily coincide with the time during the ozone hole season when the ozone column is most depleted but occur later in the year toward solstice when the solar zenith angle is smaller (Austin et al. 1994). However, observations made at Palmer station (64.5°S, 64.0°W) (McKenzie et al. 1995) have shown that the highest biologically weighted UV doses in recent years occurred there in late October in 1993, a year with particularly severe ozone loss over the Antarctic. Over southern South America, the UV irradiance during October will be additionally sensitive to the amount of ozone in the column, given the already lower solar zenith angle at these lower latitudes. A radiative transfer model (Gardiner and Martin 1996), assuming clear skies and an albedo of zero, calculated a factor 2.7 increase in erythemally weighted UV radiation at Punta Arenas for the daily average of 145.8 DU compared with the October

* Current affiliation: Defence Research Associates, Malvern, Worcestershire, United Kingdom.

Corresponding author address: Anna Jones, British Antarctic Survey, High Cross, Madingley Road, Cambridge CB3 0ET, United Kingdom.
E-mail: a.jones@bas.ac.uk

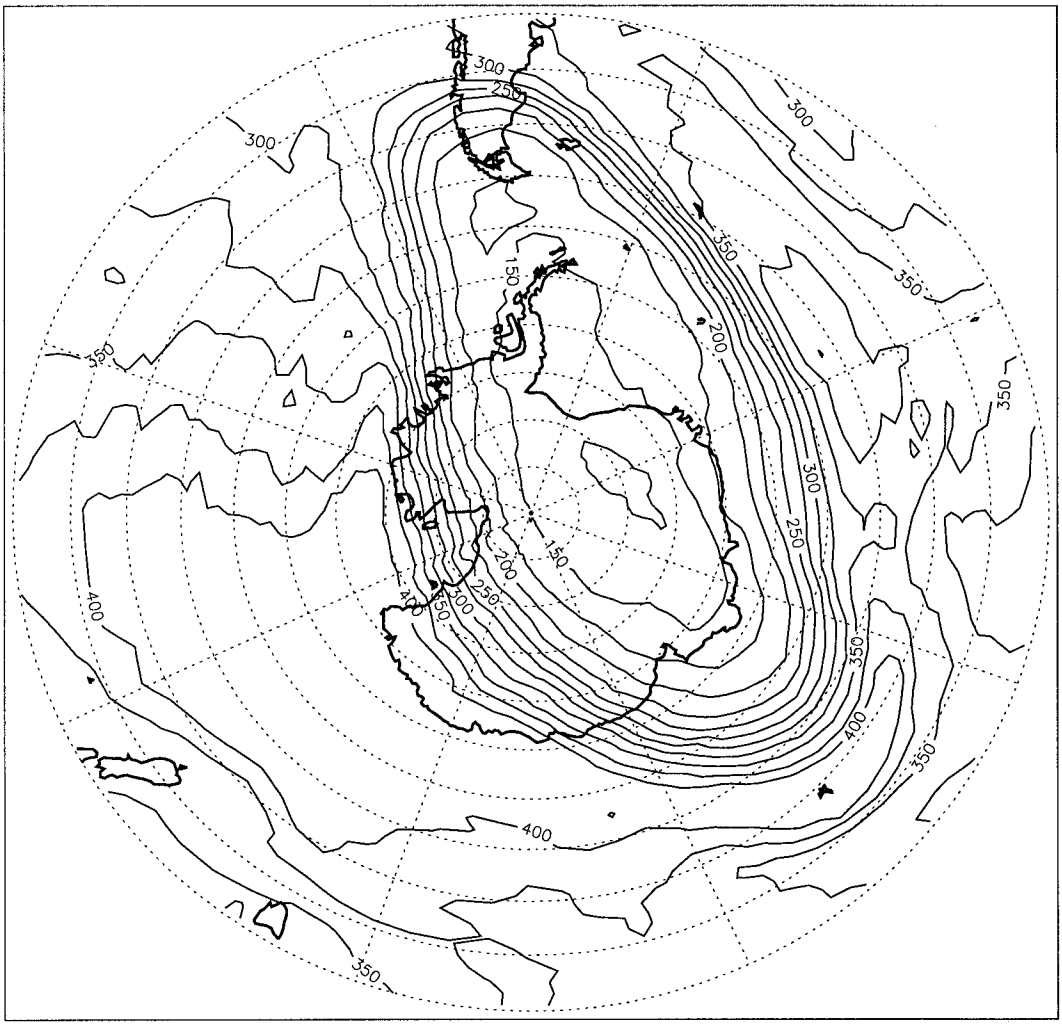

FIG. 1. TOMS observations of total ozone on 17 October 1994, showing the edge of the ozone hole over southern South America.

monthly mean of 334 DU (T. Martin 1996, personal communication). This increase is in line with derivations by Kirchhoff et al. (1996) of the increase in erythemally weighted UV radiation based on observed UV spectra at Punta, Arenas in October 1992.

Various approaches could be considered for providing a forecast of total ozone. Three-dimensional chemical modeling capabilities have increased markedly over the past few years, such that impressive work has been done to simulate observations of trace gases in the atmosphere (see, e.g., the EASOE special issue of *Geophys. Res. Lett.,* Vol. 21, No. 13, 1994; Chipperfield et al. 1995). In addition, such models have been used on occasions to make chemical forecasts, for example, when planning aircraft observing missions (Lee et al. 1997), and so, in theory, could be used to make forecasts of total ozone. Clearly, however, the problem with this approach as a general forecasting tool is that such models, and the computing resources required to run them, are not widely available.

A statistical method for forecasting total column ozone was developed by Austin et al. (1994), extending the method of Poulin and Evans (1994). Their method used 1000–250-hPa thickness fields (as a proxy for tropopause height), and temperatures at 150 and 30 hPa, and focused on the European sector of the Northern Hemisphere. For the month of September, their forecast total ozone amount compared well with observations over the United Kingdom, with a root-mean-square (rms) error of 7.4% and a mean error of 3.8%.

More recently, Stanford and Ziemke (1996) described a further method for predicting total ozone based on 50–100-hPa temperatures. They used a lookup table of a precomputed coefficient, derived from ozone climatologies from several years of satellite observations, in order to derive their ozone prediction. Focusing on the

30°–60° latitude band they generated 1-day ozone forecast errors of roughly 1%–3% (Northern Hemisphere) and 2%–3.5% (Southern Hemisphere) depending on time of year. Note, however, that when developing this method, analyzed temperature data only were used, which will favor lower ozone forecast errors than if using forecast temperatures, and also a smoothed TOMS dataset were used (5° latitude by 15° longitude). In addition, they investigated the benefit of using a multivariable model and found that the ozone prediction errors were either comparable or larger when using this technique.

In a similar manner, the method developed in this paper uses meteorological forecasts as a means of predicting total ozone. However, the aim was to produce an operational technique available for use by the scientific communities of southern South America. For this reason, we restricted ourselves to using only the most basic meteorological fields available on the World Meteorological Organization Global Telecommunications System (GTS), those of 100-hPa temperatures.

The structure of this paper is as follows. In section 2 we describe the sources of the ozone and temperature data. In section 3, the development of the forecast method is described, results of which are presented in section 4. A summary, conclusions, and a discussion of future work are given in section 5.

2. Sources of data

a. Ozone

For this analysis we use the version 7 release of total ozone data from TOMS. The data have a combined absolute and random error of ±5% under standard conditions (McPeters et al. 1996). Data are available with a resolution of 1.0° latitude by 1.25° longitude for all sunlit portions of the earth.

b. ECMWF model

Stratospheric temperatures were obtained from the European Centre for Medium-Range Weather Forecasts (ECMWF) global, operational forecast model (ECMWF 1992). This is a high-resolution spectral model with a triangular truncation of T213, giving an effective horizontal resolution of about 50 km. The vertical range is split into 31 layers, which provides detailed resolution of the vertical structure from the surface to the stratosphere. The forecast model is run in a continuous assimilation cycle, generating four analyses per day, with one 10-day forecast being produced each day from the 1200 UTC analysis. Since the ECMWF is concerned with the production of forecasts out to 10 days, the 1200 UTC analysis is prepared with a late data cutoff time of 7 h so that the vast majority of observations collected around the world are available by that time. Over Antarctica, the following data are assimilated: temperature, humidity, and winds from radiosondes and surface pressures from SYNOP messages. Satellite temperature profiles (SATEM messages) can be used to estimate layer thicknesses at a horizontal resolution of 120 km, and these data are supplied by the National Environmental Satellite, Data and Information Service. Over the ocean, SATEM thickness estimates throughout the full depth of the atmosphere are used. However, over the Antarctic continent, only stratospheric values are assimilated. In this study we have used the 1200 UTC 100-hPa temperature analyses and 48-h forecasts, with a resolution of 1.25° by 1.25°, obtained in GRIB code format. The forecasts produced by the ECMWF are the best that are currently available for the Antarctic region (Turner et al. 1996). Both 24- and 48-h 100-hPa temperature forecasts from the ECMWF model are readily available on the GTS.

3. Developing the total ozone prediction method

a. Ozone–temperature relationships

The existence of a correlation between total column ozone and certain meteorological parameters has long been recognized (Dobson and Harrison 1926). Subsequent work has focused on the observed link between total ozone and lower stratospheric temperatures [e.g., Angell (1986) and Sekiguchi (1986) for the Antarctic region during the ozone hole period]. Newman and Randel (1988) studied the correlation between monthly mean total ozone and lower stratospheric temperatures south of 40°S for the period from 1979 to 1987. They found that the highest correlations existed for temperatures in the 70–100-hPa region and that regression relationships varied from year to year.

Ozone and temperature are linked through various interrelated pathways. In addition to some limited cooling from emission in the infrared (9.6 μm), ozone is a source of heat to the stratosphere through exothermic chemical reactions that result from absorption of solar radiation. In turn, the catalytic cycles that destroy ozone are highly temperature dependent. Such reactions, together with adiabatic motion, result in the generally negative correlation between ozone and temperature in the upper stratosphere, and positive correlation in the lower stratosphere. Because the greatest concentration of ozone in the profile resides in the lower stratosphere, the total column of ozone correlates positively with lower stratospheric temperatures.

At very high southern latitudes, the ozone–temperature interrelation becomes additionally complex. The now well-known chemistry that leads to the severe springtime ozone loss over the Antarctic (Solomon 1988; WMO 1991) depends upon exposure of air parcels to low temperatures where polar stratospheric clouds may form. These clouds initiate chemical reactions and prime the Antarctic vortex for ozone destruction on the return of sunlight.

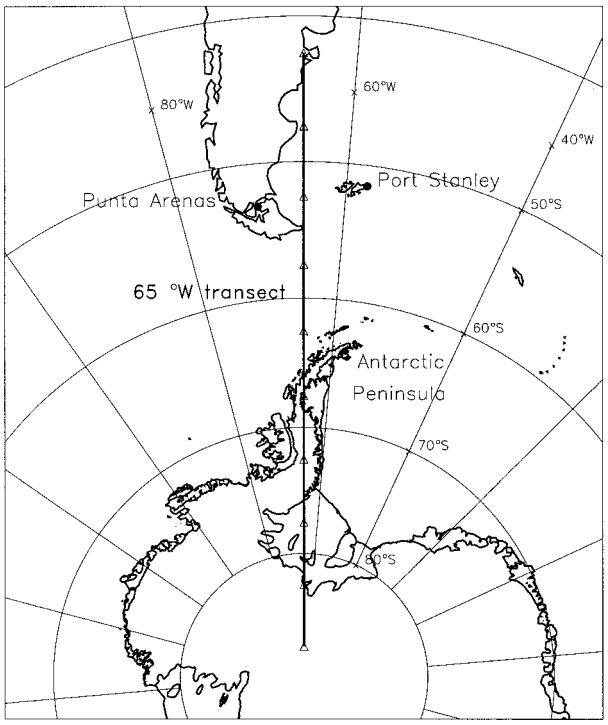

FIG. 2. Map of study area. The 65°W transect line is shown with the sample sites marked.

b. Basis for our forecasting technique

Development of the forecasting method started with an investigation into the relationship between total column ozone and 100-hPa analyzed temperatures, examining this over a transect from 42.5° to 87.5°S, centered on 65°W. This transect runs between southern Argentina and the Falkland Islands, and roughly down the Antarctic Peninsula, as shown in Fig. 2. The sampled locations along the transect lay at 5° latitude intervals, such that the grid points of the ozone and temperature data coincide exactly. We considered the period from January 1991 through October 1991. After this time the study would have been adversely affected by the sulfuric acid aerosol cloud, produced following the Mount Pinatubo eruption, that arrived in the study area in late October 1991 (Thomason et al. 1997). For each month and sample latitude, correlations between daily 100-hPa temperatures and total ozone were derived using Spearman's rank (ρ) correlation. This statistic was chosen as it does not rely upon data having a bivariate distribution, which ozone and temperature data would be unlikely to have over a month.

The temporal and spatial variability in the correlation coefficient is shown in Fig. 3. Most of the correlation coefficients are significant at the 5% level (see plot for detail), and generally all coefficients greater than 0.5 are significant at better than the 1% level. It is noticeable that the ozone–temperature correlation is less reliable where TOMS is measuring at the edge of the polar night region, which will arise partly as a result of the reduced number of ozone observations made during these months and may also reflect the somewhat larger errors in the ozone data in these regions.

Significant latitudinal and seasonal variability is evident in Fig. 3, with the correlation higher at midlatitudes and from spring to autumn, in agreement with Stanford and Ziemke (1996). For example, between

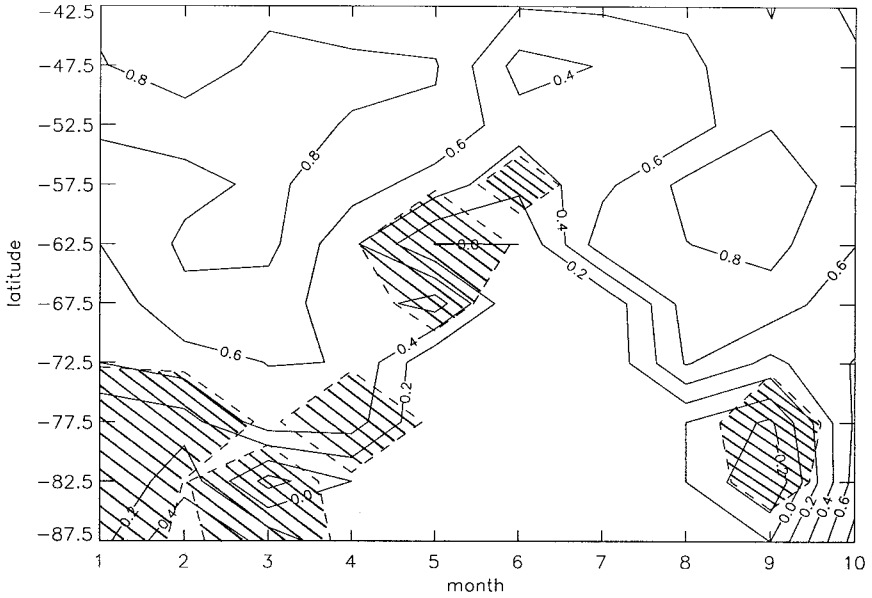

FIG. 3. Spearman's correlation coefficient (ρ) along 65°W, Jan–Oct 1991. The shaded areas denote regions that are not statistically significant at the 5% level. Note that no data are available in polar night regions.

TABLE 1. The rms daily ozone prediction error for October 1991 at 52.5°S, 65°W, where *N* is the number of previous days that the prediction was based upon.

N	rmse (DU)
7	50.7
14	34.4
21	33.3
28	34.4
35	36.6
42	37.3
49	39.7

47.5° and 52.5°S the correlation coefficient exceeds 0.8 from January to May but falls to below 0.4 during the winter. The high correlation at midlatitudes implies that a forecasting technique based upon this correlation may be considered for this region, but that it would be inappropriate at higher latitudes.

c. The prediction method

In order to forecast total ozone for a particular day, a linear regression equation relating 100-hPa temperatures (independent variable) and observed total ozone (dependent variable) was derived for the previous *N* days, where *N* varied between 7 and 49 (see Table 1). Substituting the 48-h temperature forecast into this function gave the predicted total ozone amount for 2 days' time. The regression equation thus varied from day to day, and the rms of the residuals from the regression line was the *estimated error* for the ozone prediction.

Given that we were most interested in the possibility of forecasting total ozone for the communities of southern South America, we focused our study from this point on the sample latitude of 52.5°S, which lies approximately halfway between Punta Arenas and the Falkland Islands. The choice of *N* was based upon a study of October, as this is the month when the vast majority of low ozone episodes occur at this latitude (Kirchhoff et al. 1997) and thus is of most interest to us. Forecasts were made for each day of October for each choice of *N*. The predicted total ozone was then compared with the total ozone observed for that day, and an rms error was derived (the *prediction error*). The rms prediction error for each value of *N* is given in Table 1. It is lowest, and essentially the same, for $N = 14$, $N = 21$, and $N = 28$, implying that the ozone–temperature relationship was well defined over this time envelope and not changing rapidly. Considering only the previous 7 days ($N = 7$) was clearly not long enough to derive adequately the ozone–temperature relationship. Using more than the previous 28 days progressively increased the rms prediction error, as a result of the relationship changing with time. We also investigated the prediction errors generated when using forecast 100-hPa temperatures in deriving the ozone–temperature regression equation and found that $N = 14$ gave the lowest rms prediction error for October (31.5 DU). It was thus decided to use $N = 14$ for deriving the ozone–temperature relationship for this study.

TABLE 2. The rms ozone prediction error and estimated error at 52.5°S, 65.0°W for Feb–Oct 1991. The *prediction error* is defined as the rms error derived when comparing predicted total ozone for a given day with that observed. The *estimated error* is defined as the rms of the residuals from the regression line used to forecast total ozone for a particular day. (See text for more detail.)

Month	rms prediction error (DU)	rms estimated error (DU)
Feb	15.8	9.8
Mar	16.3	10.4
Apr	20.4	18.9
May	19.9	20.5
Jun	27.5	20.8
Jul	41.0	32.1
Aug	46.7	36.3
Sep	24.3	20.6
Oct	34.4	29.6

Only linear regressions are included in this paper. The springtime data could be fitted to polynomials of greater degree, but fitting quadratic polynomials gave no appreciable improvement to the rms of the residuals or to the prediction error described in the next section.

4. Forecasting total ozone at 52.5°S

a. Comparison with observations

The rms daily ozone prediction errors and estimated errors for 52.5°S, 65°W derived using the regression relationship based upon the previous 14 days of observations, for each month between February and October 1991, are shown in Table 2. They are low for the summer months and increase progressively toward winter, in accordance with the study of Stanford and Ziemke (1996). Increased errors are associated with enhanced wave activity; in July and August an intense temperature gradient exists between mid- and high latitudes, such that the long waves are amplified; in October, enhanced dynamical activity arises from the weakening Antarctic vortex. The reasons for the increased errors are discussed below.

The daily predictions of total column ozone for September and October 1991, together with the TOMS ozone observations for these days, are shown in Figs. 4a and 4b. In September, the agreement between the predicted and the observed column ozone is very good, with the prediction method being able to reproduce the observed day-to-day variation well. The mean error for this month is 7.7 DU.

For October, the prediction method generally also does a good job, with a mean error of 14.8 DU. It predicted the low ozone episode that occurred between 4 and 6 October to within 15 DU, and that of 23 and 24 October to within roughly 20 DU. However, neither the low ozone episode of 9 October nor the minimum in ozone observed between 13 and 16 October were

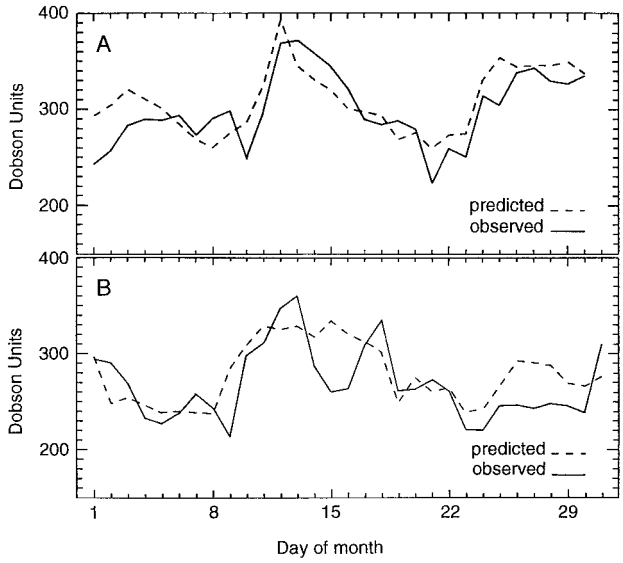

FIG. 4. Daily ozone prediction and TOMS observation for 52.5°S, 65°W for (a) September and (b) October 1991.

predicted by this method, for reasons that we will now examine.

On 8 October, a cold trough was evident in the 1200 UTC temperature analysis, centered slightly to the east of Punta Arenas (Fig. 5a). The associated minimum in ozone in the TOMS data on 8 October was centered just to the west of the South American coast (see Fig. 5b). On the following day, both low ozone and low temperatures had propagated eastward, with the low ozone values now centered roughly along the 65°W line of longitude. The error in the forecast clearly lies in the noncoincidence of the ozone and temperature troughs.

Problems with such steadily moving features might arise both from differences in timing and also from phase differences in the waves of ozone and temperature (Rood and Douglass 1985). Given that the temperature analyses are for 1200 UTC, and the TOMS observations in the Punta Arenas region correspond to roughly 1600 UTC, there will clearly be some discrepancies in sampling. During periods of intense wave activity, with steep and rapidly changing gradients of ozone and temperature, timing errors can easily be introduced into the comparison that would degrade the calculated ozone–temperature correlation. For example, timing differences would introduce a roughly 300-km error for waves of ozone and temperature traveling with a speed of 20 m s^{-1}. However, given that the ozone data in this region are always sampled a few hours after the temperature data, it would be expected that, for a coincident ozone and temperature wave, any ozone trough evident in the sampled data would lie slightly to the east of the equivalent temperature trough—the wrong sense for this example. However, another source of error lies in the tilt of the Rossby waves that is westward with altitude (Holton 1975). Given that the maximum in the ozone profile will be somewhat above 100 hPa, it could be expected that the field of integrated ozone would lie slightly to the west of any equivalent 100-hPa temperature trough, as is the case in this example. Moreover, phase shifts between the waves of ozone and temperature would be more apparent in such a relatively narrow feature than in broader waves. Forecasting such individual events is clearly challenging. From an analysis of near-simultaneous ozone and temperature fields, no consistent difference, in terms of ozone leading or lagging the temperature fields, was apparent during this season, such that no single effect was evidently dominating overall. Use of local total ozone observations, synchronized with the GTS temperature analyses, would overcome timing errors. However, the question of the influence of phase differences can only be addressed with a statistical quantification of forecast errors, based upon more than 1 year's data. This procedure is clearly necessary before this type of forecast technique can become operational.

A substantial source of error for this prediction method, however, lies in the reliability of the temperature analyses. The production of numerical weather analyses across the South Pacific is very difficult as essentially the only observational data input to the model are those derived from the TIROS Operational Vertical Sounder instrument aboard the National Oceanic and Atmospheric Administration satellites, which are relatively smoothed data. Very few ground-based measurements are made over the expanse of the Pacific Ocean. The inability of this method to forecast the ozone minimum that occurred over 52.5°S between 13 and 16 October appears to arise through a problem in the ECMWF model temperatures. Although there are substantial reductions in total ozone over this time period, as shown in the TOMS data, with a wide trough of low ozone air moving across southern South America, no such clear signal appears in the temperature data. Indeed, the temperatures are very smoothly increasing over this period (see Fig. 6). The inability of the ECMWF analyses to describe fine structure of the atmosphere over this part of the world is exemplified here. Very sharp north–south gradients of ozone are evident in the TOMS data on 13 October just off the western coast of South America. These are not apparent at all in the temperature analyses, which show very smooth east–west gradients.

b. Persistence

A further way to assess the prediction method described above is to compare the predicted total ozone with that predicted using the method of persistence. In this standard technique it is assumed that the observed quantity on a particular day will be the same as that observed on the previous day. Thus, if the forecast method has an error larger than the persistence error, it is taken to have no value. Figure 7 compares the rms prediction error at 52.5°S, 65°W derived using the persistence method with that calculated using the previous 14

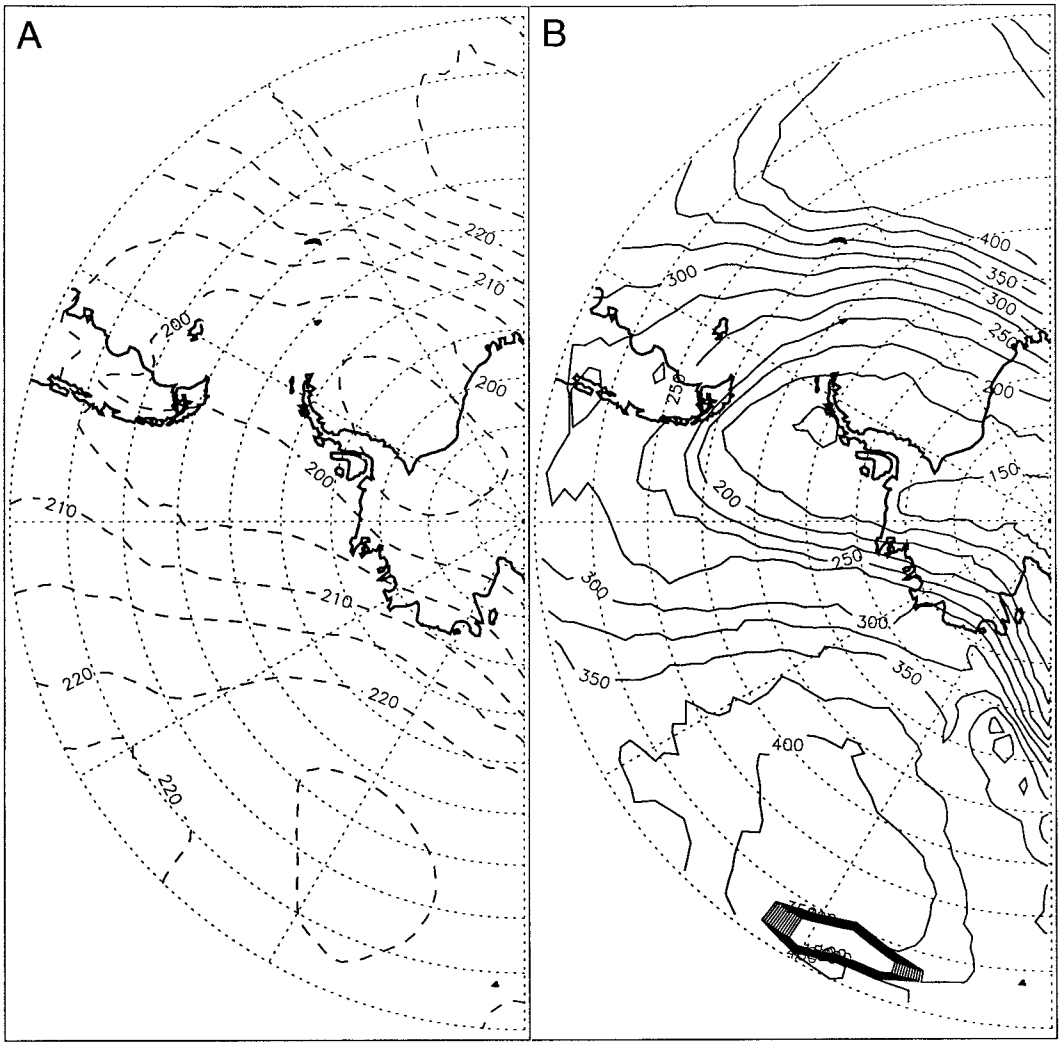

FIG. 5. (a) Map of ECMWF analyzed 100-hPa temperatures for the Punta Arenas region on 8 October 1991; (b) map of TOMS total ozone observations for the Punta Arenas region on 8 October 1991.

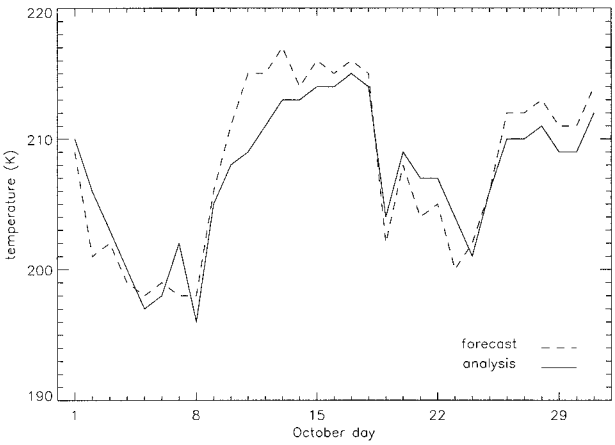

FIG. 6. Time series of daily forecast and analyzed temperatures from the ECMWF model and assimilation during October 1991 at 52.5°S, 65°W.

days of ozone and temperature data. Also shown is an extension of the persistence method: an average of the last 2 days' ozone measurements. The rms prediction error calculated by the forecasting method described here is consistently lower than either of the alternatives. For example, in October, the rms prediction error is 34.4 DU, while that for persistence is 47.0 DU.

An alternative approach to this type of prediction would be to use temperature forecasts, rather than analyses, when defining the ozone–temperature function. There will, undoubtedly, be a considerable degree of error in 48-h temperature forecast data when compared with reality. However, there might be some empirical advantage in using forecast temperatures to derive the regression function, in tandem with the forecast temperatures used in the ozone prediction. We assessed this hypothesis by predicting daily total ozone for September and October 1991, at 52.5°S, using forecast 100-hPa

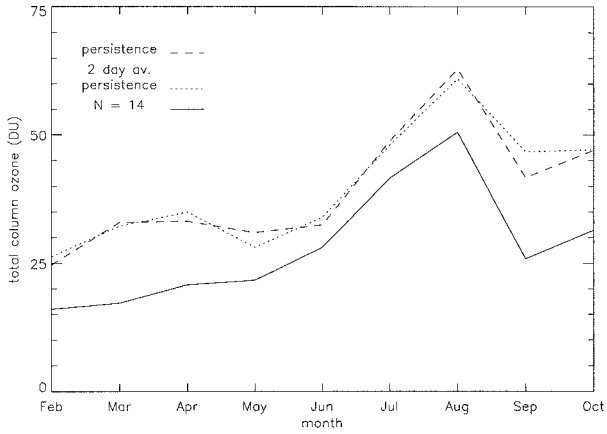

FIG. 7. The rms prediction error at 52.5°S over 1991, derived using the prediction method developed here based on the previous 14 days' ozone and temperature measurements (solid line), from the persistence method (dashed line), and from the extended persistence method (dotted line), based upon an average of the previous 2 days' measurements.

temperatures for the whole procedure. The outcome is shown in Table 3. On the whole, the results derived using the analyzed temperatures are consistently better for September, with a slightly lower rms and a lower mean error. For October, the results derived using forecast temperatures are consistently better. There thus appears to be merit in using this approach also.

5. Summary and conclusions

The aim of this work has been to assess the value in using a very simple forecasting technique that might be used to predict the periodic low ozone events that occur when the edge of the Antarctic ozone hole extends over southern South America. Under clear-sky conditions, the amount of ozone in the overhead column would be the most important parameter in determining the daily UV-B irradiance at this location and time of year. Scientists in Punta Arenas, Chile, have access to a limited number of meteorological fields via the GTS, so we restricted ourselves to using only 100-hPa temperature fields for deriving total ozone predictions.

We found that there was considerable value in this technique. In September the rms ozone prediction error was 24.3 DU, and the mean error 7.7 DU. The day-to-day variability in the predicted daily total ozone agreed well with observations during this month. In October, the month of particular interest, the rms prediction error was 34.4 DU, with the mean error 14.8 DU. The fact that the mean errors were positive in each case may be attributed to the ECMWF 100-hPa forecast temperatures tending to be too warm during these months, compared with the analysis. Two major low ozone episodes were successfully predicted to within 15–20 DU. Two further events, however, were not captured in the forecasts, highlighting potential problems should this method be used operationally.

TABLE 3. The rms daily ozone prediction error and mean error for 52.5°S, 65°W, derived using forecast temperatures in the ozone–temperature regression equation. Also shown is the persistence error (based on the previous days' observation).

Month	rms prediction error (DU)	Persistence error (DU)	Mean error (DU)
Sep	25.9	41.7	9.3
Oct	31.5	47.0	10.6

For this work to be taken further, a statistical analysis of errors arising from phase differences is necessary, which would involve examining data for several seasons. Additionally, the use of local total ozone observations, rather than satellite data, should be investigated, such that timing errors could be eliminated.

Acknowledgments. The authors wish to thank the U.K. Meteorological Office for supplying the 100-hPa temperature forecast and analysis fields from the ECMWF model, and also the TOMS ozone processing team for making their data so readily available. We are grateful also to Dr. S. Leonard, who provided valuable assistance with data manipulation and other computing problems. Very useful discussions with Prof. J. Stanford are gratefully acknowledged, as are the comments of an anonymous referee. The early stages of this work were carried out within a project funded by the U.K. Overseas Development Agency, which was concerned with ozone forecasting over southern Chile. Their support for the work is gratefully acknowledged.

REFERENCES

Angell, J. K., 1986: The close relation between Antarctic total-ozone depletion and cooling of the Antarctic low stratosphere. *Geophys. Res. Lett.,* **13,** 1240–1243.

Austin, J., B. R. Barwell, S. J. Cox, P. A. Hughes, J. R. Knight, G. Ross, and P. Sinclair, 1994: The diagnosis and forecast of clear sky ultraviolet levels at the earth's surface. *Meteor. Appl.,* **1,** 321–336.

Booth, C. R., T. B. Lucas, J. H. Morrow, C. S. Weiler, and P. A. Penhale, 1994: The United States National Science Foundation/ Antarctic Program's network for monitoring ultraviolet radiation. *Ultraviolet Radiation in Antarctic: Measurements and Biological Effects,* C. S. Weiler and P. A. Penhale, Eds., AGU Antarctic Research Series, Vol. 62, Amer. Geophys. Union, 17–37.

Chipperfield, M. P., J. A. Pyle, C. E. Blom, N. Glatthor, M. Höpfner, T. Gulde, C. Piesch, and P. Simon, 1995: The variability of $ClONO_2$ in the Arctic polar vortex: Comparison of Transall MIPAS measurements and 3D model results. *J. Geophys. Res.,* **100,** 9115–9129.

Dobson, G. M. B., and D. N. Harrison, 1926: Measurements of the amount of O_3 in the earth's atmosphere and its relation to other geophysical conditions. *Proc. Roy. Soc. London,* **110A,** 660–693.

ECMWF, 1992: ECMWF data assimilation. Research Manual 1, 3d ed., Reading, United Kingdom, 83 pp.

Gardiner, B. G., and T. J. Martin, 1996: On measuring and modelling

ultraviolet spectral irradiance. *Proc. Int. Radiation Symp.*, Fairbanks, AK, International Radiation Symposium, 317–320.

Gautier, C., G. He, S. Yang, and D. Lubin, 1994: Role of clouds and ozone on spectral ultraviolet-B radiation and biologically active uv dose over Antarctica. *Ultraviolet Radiation in Antarctica: Measurements and Biological Effects,* C. S. Weiler and P. A. Penhale, Eds., AGU Antarctic Research Series, Vol. 62, Amer. Geophys. Union, 83–91.

Holton, J. R., 1975: *The Dynamic Meteorology of the Stratosphere and Mesosphere. Meteor. Monogr.*, No. 37, Amer. Meteor. Soc., 216 pp.

Karentz, D., 1994: Ultraviolet tolerance mechanisms in Antarctic marine organisms. *Ultraviolet Radiation in Antarctica: Measurements and Biological Effects*, C. S. Weiler and P. A. Penhale, Eds., AGU Antarctic Research Series, Vol. 62, Amer. Geophys. Union, 93–110.

Kirchhoff, V. W. J. H., Y. Sahai, C. A. R. Casiccia S., F. Zamorano B., and V. Valderrama V., 1997: Observations of the 1995 ozone hole over Punta Arenas, Chile. *J. Geophys. Res.,* **102,** 16 109–16 120.

Lee, A. M., G. D. Carver, M. P. Chipperfield, and J. A. Pyle, 1997: Three-dimensional chemical forecasting: A methodology. *J. Geophys. Res.,* **102,** 3905–3919.

McKenzie, R. L., M. Blumthaler, C. R. Booth, S. B. Diaz, J. E. Frederick, T. Ito, S. Madronich, and G. Seckmeyer, 1995: Surface ultraviolet radiation. Scientific assessment of ozone depletion: 1994, World Meteorological Organization Global Ozone Research and Monitoring Project Rep. 37, 9.1–9.22.

McPeters, R. D., P. K. Bhartia, A. J. Krueger, and J. R. Herman, 1996: *Nimbus-7* Total Ozone Mapping Spectrometer (TOMS) data products user's guide. NASA Ref. Publ., NASA Scientific and Technical Information Branch, 67 pp. [Available from Global Distributed Active Archive Center, Global Change Data Center, Code 902.2, NASA/Goddard Space Flight Center, Greenbelt, MD 20771.].

Newman, P. A., and W. J. Randel, 1988: Coherent ozone-dynamical changes during the Southern Hemisphere spring, 1979–1986. *J. Geophys. Res.,* **93,** 12 585–12 606.

Poulin, L., and W. F. J. Evans, 1994: METOZ: Total ozone from meteorological parameters. *Atmos.–Ocean,* **2,** 285–297.

Sekiguchi, Y. S., 1986: Antarctic ozone change correlated to the stratospheric temperature field. *Geophys. Res. Lett.,* **13,** 1202–1205.

Setlow, R. B., 1974: The wavelengths in sunlight effective in producing skin cancer: A theoretical analysis. *Proc. Natl. Acad. Sci. U.S.A.,* **71,** 3363–3366.

Solomon, S., 1988: The mystery of the Antarctic ozone ''hole.'' *Rev. Geophys.,* **26,** 131–148.

Stanford, J. L., and J. R. Ziemke, 1996: A practical method for predicting midlatitude total column ozone from operational forecast temperature fields. *J. Geophys. Res.,* **101,** 28 796–28 773.

Thomason, L. W., L. R. Poole, and T. Deshler, 1997: A global climatology of stratospheric aerosol surface area density deduced from Stratospheric Aerosol and Gas Experiment II measurements: 1984–1994. *J. Geophys. Res.,* **102,** 8967–8976.

Turner, J., and Coauthors, 1996: The Antarctic First Regional Observing Study of the Troposphere (FROST) project. *Bull. Amer. Meteor. Soc,* **77,** 2007–2032.

WMO, 1991: Scientific assessment of ozone depletion: 1991. World Meteorological Organization Global Ozone Research and Monitoring Project Rep. 25, 271 pp.